

Measurement of the ^{13}C spin–lattice relaxation time of the non-crystalline regions of semicrystalline polymers by a cp MAS-based method

R.G. Alamo^{a,*}, J.A. Blanco^a, I. Carrilero^a, R. Fu^b

^aDepartment of Chemical Engineering, Florida Agricultural and Mechanical University and Florida State University College of Engineering, 2525 Pottsdamer St., Tallahassee, FL 32310-6046, USA

^bNational High Magnetic Field Laboratory (NHMFL), Center for Interdisciplinary Magnetic Resonance (CIMAR), 1800 East Paul Dirac Dr., Tallahassee, FL 32310, USA

Received 21 August 2001; received in revised form 5 November 2001; accepted 7 November 2001

Abstract

The non-crystalline ^{13}C spin–lattice relaxation times of atactic and isotactic polypropylene and those of an ethylene–1-octene copolymer of low crystallinity have been measured by classical inversion and saturation recovery methods as well as by a cp MAS-based pulse sequence. The latter is a saturation recovery-type sequence that involves cross-polarization. It samples preferentially the soft non-crystalline regions of semicrystalline polymers. The method is found to be useful in determining $T_{1\text{C}}$ of the amorphous regions of semicrystalline iPP at room temperature. It is found that the atactic PP molecule and the non-crystalline iPP regions have the same average segmental relaxation rate. The $T_{1\text{C}}$ of some of the carbons investigated was $<T_{1\text{H}}$ and the experimental recovery curves showed complex exponential behavior from the contribution of a transient nuclear Overhauser effect (NOE) to the ^{13}C magnetization. Moreover, the experimental data were fitted with a double exponential function obtained from solving the Solomon equations. The fitting leads to $T_{1\text{C}}$ in very good agreement with the values obtained by classical inversion or saturation recovery sequences. The same $T_{1\text{C}}$ value was obtained with the cp-based sequence when transient NOEs were eliminated by saturation of the proton magnetization during the delay period. The hexyl branches of the ethylene copolymer lead to an increased average backbone C–C intermolecular distance in the non-crystalline regions compared to those of the linear polyethylene chain and, thus, to a higher backbone methylene segmental mobility. © 2002 Elsevier Science Ltd. All rights reserved.

Keywords: NMR in solids; Spin–lattice relaxation; Isotactic polypropylene

1. Introduction

The ^{13}C spin–lattice relaxation of the crystalline and liquid-like regions of semicrystalline polymers, such as the polyethylenes and polypropylenes usually differ in two or three orders of magnitude [1,2]. Thus, the measurement of this relaxation time is customarily done with different pulsing programs. While the sequence devised by Torchia [3] is preferred to determine T_1 (^{13}C) of the crystalline region, a classical saturation recovery sequence has been used to probe the T_1 (^{13}C) of the highly mobile amorphous regions [3–5]. Whenever possible, proton enhanced ^{13}C induction via the cross-polarization (cp) process is desired because it relies on the abundant ^1H spins and gives rise to an increased signal amplitude relative to the single pulse sequence. In addition, since the recycle period in a cp experiment is dictated by the ^1H spin–lattice relaxation

which is usually much shorter than that of ^{13}C , the length of the measurement can also be considerably shortened.

The Torchia sequence has been used to measure long T_1 (^{13}C) of the crystalline regions of isotactic polypropylene [6] and linear and branched polyethylenes [5,7]. Saturation and inversion recovery are used to probe T_1 (^{13}C) of the non-crystalline phase [5,6,8]. VanderHart has also used a (180-10s-90-10s)x sequence to isolate the ^{13}C signal of the non-crystalline component of drawn and undrawn linear polyethylene [9]. As in a saturation or inversion recovery sequence, no cross-polarization is involved in the latest method and therefore, they do not provide the benefit of increasing magnetization of molecular carbons that have low amplitude. For example, the limited amplitude of motion of the non-crystalline regions of isotactic polypropylene makes it difficult to isolate the recovery of the carbon magnetization in this region. Hence, in an earlier work, the T_1 (^{13}C) for CH_2 and CH of isotactic polypropylenes were only measured at temperatures above ambient conditions to increase their mobility [6].

* Corresponding author.

E-mail address: alamo@eng.fsu.edu (R.G. Alamo).

Table 1
Characterization of polymers studied

Sample designation	Polymer type	M_w (g/mol)	M_w/M_n
APP ^a	Atactic polypropylene	190,000	1.1
Z-iPP-160	Isotactic polypropylene, 0.86 mol% stereo defects	271,500	6.1
EO12.6-Q	Random ethylene–1-octene copolymer, 12.6 mol% 1-octene	142,800	2.1

^a Hydrogenated poly(2-methyl-1,3-pentadiene).

We report in this communication a saturation recovery type of method that invokes cross-polarization. It is based on a pulse sequence that selects the more mobile component from the difference in spin–lattice relaxation time of the crystalline and the non-crystalline regions. The method improves intensity signal and facilitates measurement of T_1 (^{13}C) of non-crystalline carbons of low amplitude. Moreover, to avoid possible overlaps in the relaxation of the liquid-like and interfacial regions, the method is first tested using a model atactic polypropylene. This is a completely amorphous material in contrast to commercial atactic polypropylenes that show some crystallinity. The results are compared to those obtained using the standard saturation recovery sequence. In the course of the study, the magnetization of the CH_3 group of atactic polypropylene was shown to be affected by a transient nuclear Overhauser effect (NOE) because $T_{1\text{C}} < T_{1\text{H}}$ for this group. The experimental spin–lattice relaxation of the CH_3 group was modeled to a double exponential process that includes a ^1H – ^{13}C cross-relaxation. The carbon magnetization recovers as a single-exponential process via saturation of the ^1H -initial magnetization.

A comparison of the cp-based method and saturation recovery is also undertaken using a semicrystalline polypropylene and a linear low density polyethylene. The spin–lattice relaxation properties at room temperature of the atactic polypropylene and the amorphous regions of semicrystalline iPP are directly compared.

2. Experimental part

The polymers studied in this work are listed in Table 1. The hydrogenated poly(2-methyl-1,3-pentadiene) is a model sample for atactic polypropylenes (APP). It was synthesized following a method devised by Fetters [10]. The high resolution ^{13}C NMR spectrum of an identical APP of lower molecular weight was reported by Sakurai et al. [11]. While the methine resonance is quite narrow, the methyl and methylene are much broader. These features have been associated with different degrees of intermolecular perturbations. The methine resonance is narrow because the methine carbon is most shielded in the interior of the backbone conformation. Sample Z-iPP-160 is an unfractionated Ziegler-type isotactic polypropylene that was crystallized at 160 °C for 90 days. To prevent oxidation

during the long crystallization time, the sample was vacuum-sealed in a glass tube. The crystallinity of this sample, measured by WAXS is $\sim 70\%$ and the DSC peak melting temperature is 185 °C. The third sample listed in Table 1 is an ethylene–1-octene random copolymer made with a metallocene catalyst [12]. It contains 12 mol% of 1-octene and a small amount of long chain branching. The molecular weight and comonomer content distributions are both narrow for this copolymer. A film ca. 0.2 mm thick was prepared by compression molding in a Carver Press at 150 °C for 2 min and further quenched in water at 25 °C. The DSC degree of crystallinity and melting peak are 8% (based on a heat of fusion for the pure PE crystal of 290 J/g) and 60 °C, respectively.

All the solid state NMR experiments were carried out on a Bruker DMX300 spectrometer operating at 75.5 MHz for ^{13}C and at 300.2 MHz for ^1H . The experiments were conducted at room temperature using a Bruker solid-state probe for 7 mm rotors. The magic angle spinning (MAS) frequency was 3000 ± 500 Hz. The nutation frequencies associated with the ^{13}C and ^1H radio frequency fields were 55 and 50 kHz, respectively. A contact time of 500 μs was used in the cp MAS experiments. Signal averaging was collected using 250–500 scans depending on the pulse sequence used.

3. Results and discussion

The single pulse ^{13}C NMR spectrum of APP obtained under MAS and high power decoupling with a recycle delay of 12 s is shown in Fig. 1(a). Resonances of the methyl, methine and methylene carbons appear at 21 (sharp), ~ 27 (broad) and ~ 47 ppm (broad), respectively. It is interesting that the resonance of the methyl carbon is relatively sharp indicating the fast internal rotation of the group relative to the other two carbons. The relative intensities of the methine and methyl carbons in the spectrum of the solid are reversed compared to the ratio found in the solution spectrum [11] and resemble the non-crystalline spectrum obtained by subtracting two cp MAS spectra of a semicrystalline iPP under different spin locking times of the ^1H polarization, prior to contact [13]. The low intensity, broad peaks of the methylene and methine carbons reveal the slow segmental motions of the APP molecule, whereas the motion of the methyl carbons is dominated by their

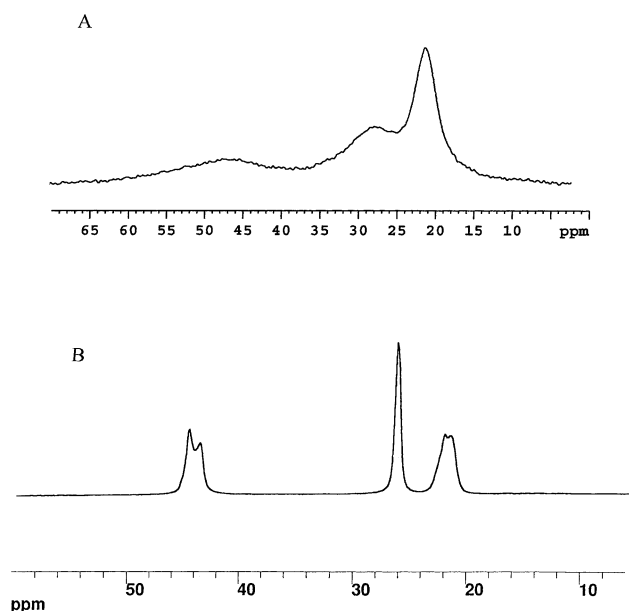


Fig. 1. (a) Single pulse spectrum of APP with a 12 s recycle time; (b) cp MAS spectrum of slowly cooled Z-iPP.

internal rotation. Broader peaks in the amorphous spectrum, compared to the spectrum of the crystalline sample, are normally associated with less ordered chains [13]. In contrast, as seen in Fig. 1(b), the cp MAS spectrum of semicrystalline iPP (crystallized in pure alpha phase), is characterized by sharp narrow lines. The splitting of the methyl and methylene lines is associated with dissimilar intermolecular interactions along the helix in the monoclinic packing [14]. Resonances characteristic of the amorphous regions are not sharp and are only indicated as broad components in the spectrum of the semicrystalline sample [6]. Thus, differences in chemical shifts between the carbons of the crystalline and non-crystalline regions are observed at temperatures greater than $\sim 60^\circ\text{C}$ as small resonances shifted about 2 ppm to low fields from the CH_2 and CH crystalline resonance lines [6]. Resonances assigned to the amorphous regions are only apparent in the room temperature spectra as a broad shoulder to the methylene and methyne resonances consistent with the broad lines of the APP spectrum of Fig. 1(a).

The low intensity of the non-crystalline CH_2 and CH magnetization reveals that investigating the relaxation of these groups in the semicrystalline iPP it is desired and important to enhance their magnetization via cross-polarization. For example, the ^{13}C spin–lattice relaxation time ($T_{1\text{C}}$) of the methylene or methine carbons in the amorphous regions is one of the properties that gives information about possible conformational changes of segmental groups in this region during aging or isothermal annealing of the initially formed crystallites. The $T_{1\text{C}}$ measurement via cross-polarization will improve resolution in the experimental measurement to better resolve the dynamics of the non-crystalline regions during annealing. Thus, changes in

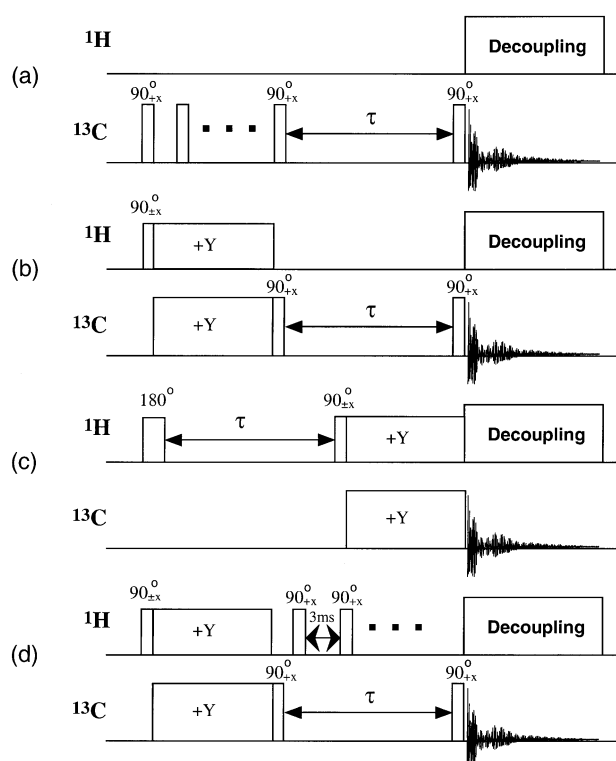


Fig. 2. NMR pulse sequences used in this work: (a) saturation recovery for $T_{1\text{C}}$ measurement; (b) sequence for selection of short $T_{1\text{C}}$ with cross-polarization; (c) sequence for $T_{1\text{H}}$ measurement; (d) same as (b) with proton saturation during recovery.

thermal properties of polyolefins during annealing have been associated with segmental reorganization and a decrease in the molar conformational entropy in the amorphous regions [15]. The $T_{1\text{C}}$ measurement probes segmental relaxation and therefore, gives an indirect measurement of possible conformational changes.

As a reference, the purely non-crystalline polypropylene was first analyzed. The ^{13}C spin–lattice relaxation of the three types of carbons of APP were obtained using the standard saturation recovery method given schematically in Fig. 2(a). A train of 26, 90° pulses was applied to the carbon channel separated by equal intervals of 20 ms each to saturate the magnetization. Between 21 and 28 delay times (τ) were used to determine the magnetization recovery curves. Acquisition was obtained under high power decoupling (60 kHz) with a recycle time of 3 s. The results of single exponential fittings are listed in Table 2. $T_{1\text{C}}$ values of 1.18, >1.35 and 0.67 s were obtained for CH_2 , CH and CH_3 , respectively. Also listed in this table are extrapolated data at room temperature from the $T_{1\text{C}}$ -temperature studies of Moe et al. [8] obtained at 75.4 MHz for a similar atactic polypropylene. These authors used the inversion recovery sequence to obtain $T_{1\text{C}}$. The agreement is excellent in spite of the different molecular weights of the polypropylenes. The M_w of the sample analyzed by Moe et al. is 31,000 g/mol, a value significantly lower than the 191,000 g/mol of the APP used in this study. This agreement indicates that at room

Table 2
 ^{13}C spin–lattice relaxation times obtained for APP using different pulsing methods

Pulsing method	CH ₂ (s)	CH (s)	CH ₃ (s)
Saturation recovery	1.18	1.35 ^a	0.67
Inversion-recovery (Moe et al. [8])	1.2	1.6	0.7
cp MAS (sequence 2b)	1.1	1.4	0.56 ^b
cp MAS, ^1H saturation (sequence 2d)	1.19	1.61	0.64

^a Magnetization was not fully recovered, hence the $T_{1\text{C}}$ value was underestimated.

^b Obtained from the fitting with Eq. (3).

temperature, the segmental motions of the two atactic polypropylene chains are the same.

The spin–lattice relaxation of APP was further obtained using a method derived from the Torchia sequence [3] that invokes cross-polarization, as shown in Fig. 2(b). After the ^{13}C magnetization is enhanced by cross-polarization, it is flipped to the $-z$ axis by a $+90^\circ$ pulse. After a variable delay τ during which the ^{13}C magnetization recovers towards equilibrium, the magnetization is examined by applying a second $+90^\circ$ pulse. In a following consecutive experiment, after cross-polarization, the carbon magnetization is rotated to the $+z$ axis, followed by the same variable delay τ and $+90^\circ$ pulse to record the magnetization. When the variable delays are constrained to relatively short times, those relevant to the amorphous regions, the sum of the signals from consecutive experiments makes null the magnetization of the slow relaxing crystalline carbons and recovers, with increasing delay time, the magnetization of the non-crystalline component. Therefore, the $T_{1\text{C}}$ sequence of Fig. 2(b) is a saturation recovery-based sequence, preferential for soft regions, that involves cross-polarization.

The experimentally measured intensity enhancement in the cp experiment was approximately 2.5 for the APP sample. The recovery curves obtained with the cp sequence (2b) are shown in Fig. 3. It is clear that the magnetization for CH₂ and CH groups follows the expected saturation recovery curve. However, transient NOE are evident in the course of the saturation recovery of the methyl carbon [16,17]. A single exponential fitting of the recovery of the magnetization for CH₂ and CH that are not affected by the transient NOE leads to basically identical $T_{1\text{C}}$ values to those obtained from saturation recovery (1.1 and 1.4 s, respectively). The transient NOE effect is significant when $T_{1\text{C}} \leq T_{1\text{H}}$ and has been shown to lead to multi-exponential spin–lattice relaxations of the type shown in Fig. 3, for the methyl groups of a variety of organic solids [17–20]. To document that a transient NOE was affecting the magnetization of the methyl group and had no effect on the methine and methylene groups, the $T_{1\text{H}}$ of the APP was measured following the standard pulse sequence given in Fig. 2(c). Due to fast spin diffusion, an average value of 0.77 s was obtained for all types of protons. This value is higher than the $T_{1\text{C}}$ for the

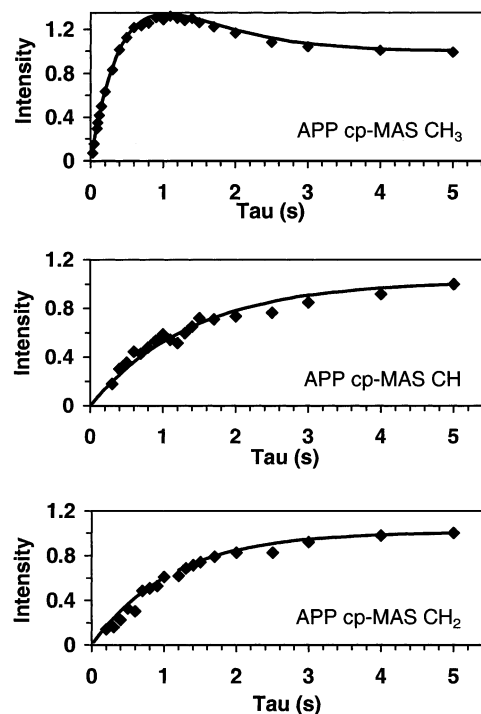


Fig. 3. Experimental spin–lattice relaxation curves for the three ^{13}C resonances of APP obtained using sequence 2(b). Note the contribution of a transient NOE in the recovery of the CH₃ magnetization. Fittings with Eq. (3) (top) and Eq. (4) (middle and lower recoveries) are indicated as solid lines.

methyl group listed in Table 2, and demonstrates that the methyl group of APP may be subject to a transient NOE effect. The experimental curves for the methylene and methine carbons obey $T_{1\text{C}} > T_{1\text{H}}$ and thus show normal relaxation behavior.

In an attempt to compute the methyl $T_{1\text{C}}$, the experimental result shown in Fig. (3) for the CH₃ group was modeled according to the Solomon equations. These equations describe the spin–lattice relaxation process for a heteronuclear two-spin system [4,21]. Denoting S (^{13}C) the dilute spins and I (^1H) the abundant spins, their relaxation is governed by the following pair of differential equations:

$$\frac{dS_{z(t)}}{dt} = -\frac{1}{T_{1\text{C}}}[S_{z(t)} - S_{z(\text{eq})}] - \frac{1}{T_{1\text{CH}}}[I_{z(t)} - I_{z(\text{eq})}] \quad (1)$$

$$\frac{dI_{z(t)}}{dt} = -\frac{1}{T_{1\text{HC}}}[S_{z(t)} - S_{z(\text{eq})}] - \frac{1}{T_{1\text{H}}}[I_{z(t)} - I_{z(\text{eq})}] \quad (2)$$

where $I_{z(t)}$ and $S_{z(t)}$ are the magnetizations at a given time t and $I_{z(\text{eq})}$ and $S_{z(\text{eq})}$ are the corresponding equilibrium values.

For the very dilute ^{13}C spins of our system, the cross-relaxation rate from the ^{13}C spins to the abundant ^1H spins, given as $1/T_{1\text{HC}}$, is negligible and the analytical solutions of Eqs. (1) and (2), with boundaries from the initial magnetization $I_{z(0)}$ and $S_{z(0)}$ to the equilibrium values, after two consecutive experiments, lead to the following

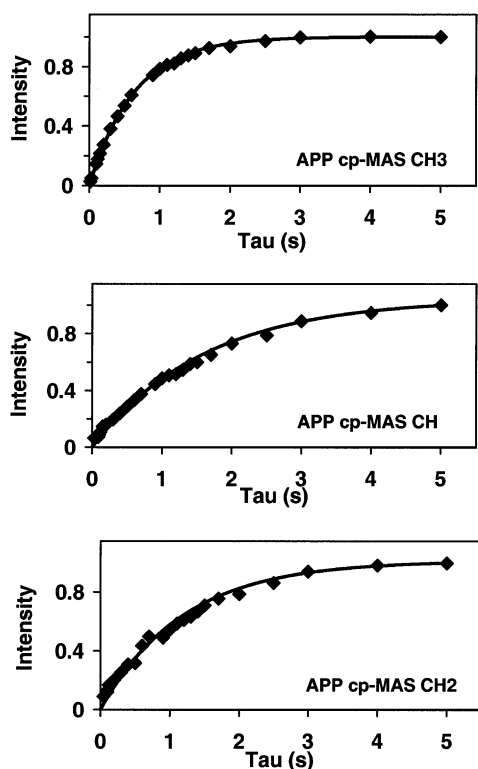


Fig. 4. Experimental spin–lattice relaxation curves for the three ^{13}C resonances of APP obtained using sequence 2(d), cp MAS with proton saturation. Fitting to single exponential functions are given by the solid line.

expression for the carbon magnetization:

$$\frac{S_{z(t)}}{2S_{z(\text{eq})}} = 1 + \frac{\eta}{\left(1 - \frac{T_{1\text{C}}}{T_{1\text{H}}}\right)} \exp\left(-\frac{t}{T_{1\text{H}}}\right) - \left[1 + \frac{\eta}{\left(1 - \frac{T_{1\text{C}}}{T_{1\text{H}}}\right)}\right] \exp\left(-\frac{t}{T_{1\text{C}}}\right) \quad (3)$$

The ratio between the longitudinal relaxation rate ($1/T_{1\text{C}}$) and the cross-relaxation rate between the S and I coupled spins ($1/T_{1\text{CH}}$) defines the NOE factor $\eta = \gamma_{\text{H}}T_{1\text{C}}/\gamma_{\text{C}}T_{1\text{CH}}$.

γ_{H} and γ_{C} are the corresponding gyromagnetic constants. Eq. (3) reduces to the expression for an isolated spin system in the absence of cross-relaxation

$$S_{z(t)} = (S_{z(0)} - S_{z(\text{eq})})\exp\left(-\frac{t}{T_{1\text{C}}}\right) + S_{z(\text{eq})} \quad (4)$$

A fitting of the experimental ^{13}C magnetization (CH_3) with Eq. (3), with $S_{z(\text{eq})}$, $T_{1\text{C}}$ and η as adjustable parameters, leads to values for the methyl spin–lattice relaxation and NOE factor of 0.56 s and 1.32, respectively. A good fitting of the experimental data, shown by the continuous line of the top plot in Fig. 3, confirms the cross-relaxation effect during recovery and the calculated $T_{1\text{CH}}$ is 1.7 s. As seen in Table 2, the calculated $T_{1\text{C}}$ is very close to the value

obtained from saturation or inversion recovery, indicating that the simplified solution of the Solomon equations, given by Eq. (3), can be used to find $T_{1\text{C}}$ values from the multi-exponential experimental recovery curve. The value for the NOE factor of the methyl group of APP is typical of carbons of similar types in other polymers, for example, NOE factors of ~ 1.37 were found for the CH_3 groups of polyisobutylene at 67.9 MHz [22].

The approach to eliminate the transient NOE effect is to saturate the proton resonances during the $T_{1\text{C}}$ measurement by using r.f. irradiation that is very weak in comparison with the decoupling r.f. field [17]. The pulse sequence is shown in Fig. 2(d). A train of 90° pulses with 3 ms equal intervals is applied to the proton channel. The experimental magnetization recovery curves obtained with this sequence are shown in Fig. 4. The magnetization curves for the three types of carbons, obtained with proton saturation, show enhanced intensities and single exponential recoveries. A fitting with Eq. (4) is also shown in this figure and leads to $T_{1\text{C}}$ of 1.19 s (CH_2), 1.61 s (CH) and 0.64 s (CH_3). As seen in Table 2 these values are in perfect agreement with the $T_{1\text{C}}$ values obtained via saturation or inversion recovery.

A test of intensity enhancement through the use of sequence (b) of Fig. 2, to probe $T_{1\text{C}}$ of the carbons in the non-crystalline regions of semicrystalline polypropylenes was carried out with sample Z-iPP-160. This polypropylene of high isotacticity content developed $\sim 70\%$ crystallinity after longtime crystallization at 160°C . Hence, the non-crystalline content is only about 30%. The intensity of the methylene and methine NMR signals obtained with the cp sequence increased compared to the saturation recovery method and led to spectra with improved signal/noise ratio. Comparative examples are shown in Fig. 5. Fig. 5(A) shows a series of spectra, at selected delay time values, obtained by saturation recovery. The non-crystalline CH_2 resonance (40–50 ppm) is broad and of low intensity reflecting the low amplitude of motion and the low fractional content of this region in the sample analyzed. For delay times greater than 7 s, it remains buried within a sharper resonance corresponding to more ordered CH_2 , those typical of the interphase or crystalline regions. The broad non-crystalline CH_2 resonance was indistinguishable from the background noise in the spectra obtained with delay times shorter than 0.5 s. It is also evident that the low amplitude of this resonance and the high noise level lead to high uncertainties ($\sim 40\%$) in the measured $T_{1\text{C}}$ value for the non-crystalline CH_2 with this method. Representative spectra after short delay times using the cp MAS-based sequence (b) of Fig. 2 are shown in Fig. 5(B). It is clear that the non-crystalline CH_2 resonance is resolved even at very short delay times (0.15 s) and the experimental error in the measurement was significantly decreased ($\pm 20\%$). This resonance was deconvoluted from the overlapping resonance corresponding to more ordered conformations using as reference the line-shape of the room temperature APP spectrum. The expanded inserts in Fig. 5

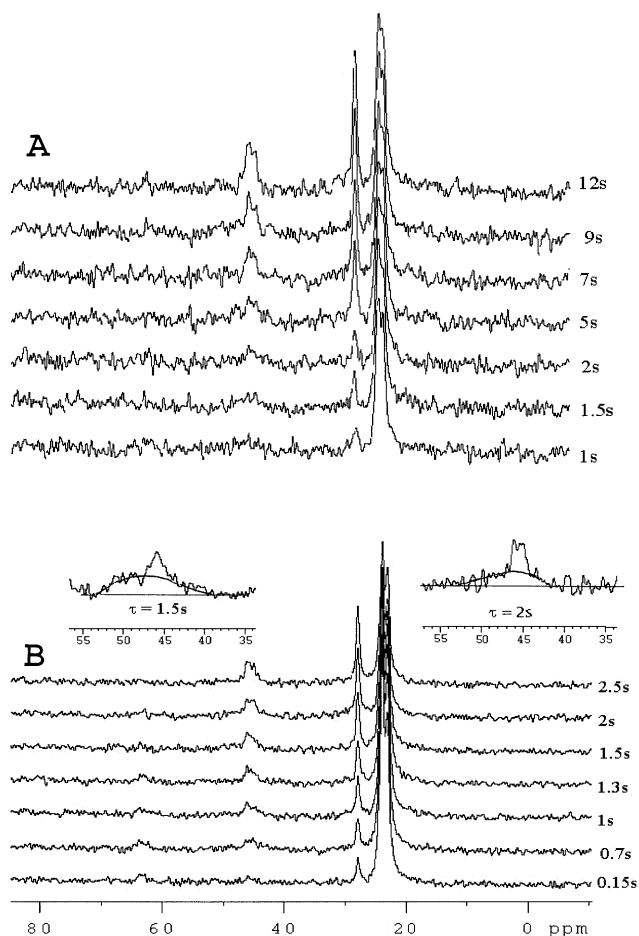


Fig. 5. Spectra of Z-iPP-160 at the indicated delay times obtained by saturation recovery following sequence 2(a), series (A) and cp MAS-based sequence 2(b), series (B). The 35–55 ppm region is expanded in the right insert to illustrate the deconvolution of the non-crystalline component. The left insert is an example for a rapidly crystallized iPP for which the non-crystalline fraction is significantly higher and thus, it is better resolved as shown.

show examples of this deconvolution. The values for the methyl T_{1C} are obtained with the lowest degree of uncertainty from both methods (<5%). Within the above uncertainties, saturation recovery and the cp MAS-based method led to the same T_{1C} values, which are listed for the three types of carbons in Table 3. These results show evidence that the cp method may be used to increase the sensitivity of the measurement of the relaxation behavior of the non-crystalline component.

The T_{1C} for the methylene groups of the non-crystalline region has a value of 1.25 s. This value is only slightly higher than the value obtained for the pure atactic polypropylene of 1.20 s, indicating that the mixed conformations of the isotactic molecule in the non-crystalline region average the same segmental relaxation as the atactic molecule with absolute random stereochemistry. One could question if the similarity of T_{1C} between the APP and the non-crystalline iPP is a consequence of the heterogeneous molecular microstructure of the Ziegler iPP studied. Heterogeneous Ziegler type catalysts leave a fraction of atactic component in the iPP and a non-uniform distribution of the chain isotacticity, i.e. the non-isotactic content is usually concentrated in the low molecular weight chains [23]. Since both atactic and highly defective, non-crystallizing chains are concentrated in the non-crystalline region of the iPP material; the average conformations in this region may approach that of the pure APP. However, additional experiments using homogeneous metallocene type polypropylenes in which the atactic component was removed, led to the same T_{1C} values for the non-crystalline carbons as those obtained for the APP and for the Ziegler type [24]. The stereochemistry of the metallocene type molecules in the non-crystalline region should be quite different from that of the APP, yet they have the same segmental relaxations at room temperature. The T_{1C} of the CH_3 group of the atactic and semicrystalline (non-crystalline region) iPP are also

Table 3

^{13}C spin–lattice relaxation times for the non-crystalline regions of isotactic polypropylene and ethylene–octene copolymer. Data obtained using saturation recovery and the cp MAS-based saturation recovery

Z-iPP-160						
Pulsing method	CH ₂ (s)	CH (s)	CH ₃ (s)			
Saturation recovery	1.27	1.82 ^a	0.47			
cp MAS (sequence 2b)	1.25	1.20 ^a	– ^b			
EO12.6-Q						
	CH ₂ (α to CH) (s) (~35 ppm)	CH ₂ (β to CH ₃) (s) (~33.5 ppm)	CH ₂ backbone (s) (~31 ppm)	CH ₂ (β to CH) (s) (~28 ppm)	CH ₂ (α to br-CH ₃) (s) (~24 ppm)	Branch CH ₃ (s) (~15 ppm)
Saturation recovery	0.25	0.43	0.27	0.21	0.52	1.32
cp MAS (sequence 2b)	0.17 (0.96) ^c	0.39 (1.00) ^c	0.29 (1.17) ^c	0.23 (1.00) ^c	0.53 (1.12) ^c	1.31
cp MAS, ¹ H saturation (sequence 2d)	0.21	0.40	0.28	0.21	0.54	1.46

^a Underestimated value. The magnetization was only partially recovered.

^b Sample was not run with proton saturation (sequence d of Fig. 2), and complex transient NOE effects during recovery of the amorphous and crystalline CH₃ magnetization are present.

^c T_{1C} and NOE factors obtained from fitting with Eq. (3). The NOE factors are given in parenthesis.

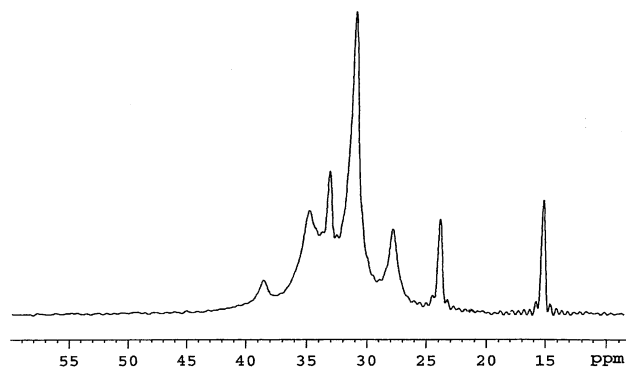


Fig. 6. Single pulse spectrum of EO12.6-Q obtained with 12 s recycle time. See text for assignments.

similar and in good agreement with the value of 0.51 s, given by Gomez et al. [25] for this group, confirming the motional similarity of amorphous iPP and the atactic polymer at room temperature. These results parallel the studies by Komorowski et al. [26] who found the T_{1C} of the non-crystalline regions of linear and branched polyethylenes at ambient temperature to be independent of the crystallinity level. Thus, the fast segmental motions at, or near, the nuclear Larmor frequency of 5–500 MHz, that determine T_{1C} , must be the same for the non-crystalline regions of iPP and those of the amorphous atactic sample, reflecting a similar type of chain structure. In addition, these NMR experiments confirm other results by neutron scattering which indicated that, upon solidification of flexible chains, the random conformation was preserved in the amorphous regions [27].

The experimental T_{1C} values listed in Tables 2 and 3 are consistent within the different pulsing techniques used in our work and with the data of Moe et al. [8]. The values are, however, significantly higher than those reported by Saito et al. [6] for isotactic polypropylene crystallized at 140 °C. Room temperature values for the non-crystalline methylene and methine groups were not listed in their work and a value of 0.27 s was given for the methyl T_{1C} . At 64 °C, the non-crystalline methylene T_{1C} was reported as <0.2 s and the value for methine as ~0.3 s. We cannot explain the discrepancy with our data except perhaps for the fact that the measurements of Saito et al. were carried out at a higher temperature.

The cp MAS-based saturation recovery method was also used to measure T_{1C} of different non-crystallizable carbons of the ethylene–1-octene copolymer listed in Table 1, and the values were compared with those obtained from the standard saturation recovery method. The single pulse spectrum obtained with a recycle delay of 12 s is given in Fig. 6. About 90% of this copolymer is amorphous allowing resolution of up to seven different types of carbons from the backbone and the branch. In reference to the high resolution solution spectrum [28], we assign resonances at ~15 ppm (CH_3), ~24 ppm (CH_2 α to CH_3), ~28 ppm (CH_2 β to CH), ~31 ppm (backbone CH_2), ~33.5 ppm (CH_2 β to CH_3),

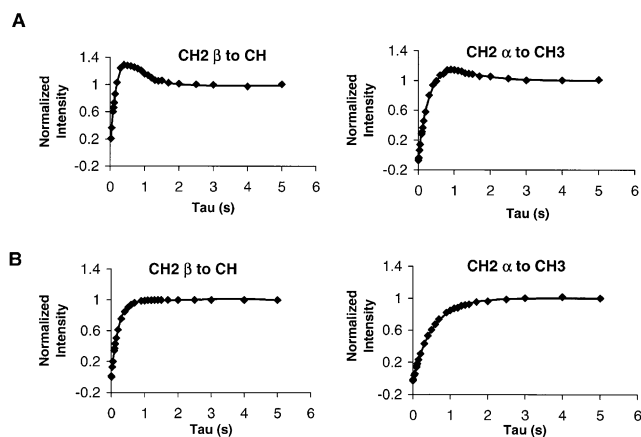


Fig. 7. (A) Experimental spin–lattice relaxation curves for CH_2 (α to CH_3) and CH_2 (β to CH) in EO12.6-Q obtained using sequence 2(b); (B) same after proton saturation following sequence 2(d). The solid lines are the corresponding fittings with Eq. (3) (top) and single exponential fittings according to Eq. (4) (bottom).

~35 ppm (CH_2 α to CH) and ~38.5 ppm (CH). With a delay of 12 s and considering that this sample is of low crystallinity, the crystalline CH_2 is only indicated as a broad shoulder in the low field region of the main CH_2 resonance in Fig. 6. The T_{1C} measured by different NMR sequences are listed in Table 3. The T_{1H} of this copolymer was measured with sequence (2c) and averages, for all the different molecular protons, 0.45 s. Except for the methyl carbon of the hexyl branch, the T_{1C} of any other non-crystalline carbon, measured by saturation recovery, is similar or less than 0.45 s. Consequently, the cp MAS based T_{1C} curves obtained with sequence (2b) show complex recoveries from a transient NOE effect. The experimental multi-exponential recoveries are nevertheless, well fitted with Eq. (3). As examples, the experimental recovery curves and theoretical fitting according to Eqs. (3) and (4) for the 24 ppm CH_2 (α to CH_3 of the branch) and the 28 ppm CH_2 (β to CH) magnetization are given in Fig. 7. Data were obtained with the cp MAS pulse sequence without (Fig. 7(A)) and with proton saturation (Fig. 7(B)). From the fitting with Eq. (3), NOE factors of 1.12 and 1.0 were calculated in agreement with other experimentally obtained values for the non-crystalline regions of linear polyethylene (1–1.5) [22]. The methylene T_{1C} obtained from this fitting are, as seen in Table 3, the same as those obtained by saturation recovery or by cp MAS with proton saturation. Listed in Table 3 are results for the non-crystalline backbone methylene carbon, the branch methyl carbon, methylenes α and β to the methyl of the branch and methylenes α and β to the methine carbon. The uncertainties of the T_{1C} values are relatively low, 3–5%. Agreement between the different methods of analysis, including the simplified model of the magnetization recovery after cross-polarization given by Eq. (3), is excellent. The relatively high T_{1C} value for CH_3 (~1.4 s) compared to the ~0.25 s of the backbone and

inner branch methylenes, indicates that the relaxation of the CH₃ group of the hexyl branch is in the fast motional region. The fast internal molecular relaxation of this group also propagates to the adjacent α and β CH₂ groups as per their higher T_{1C} values (0.53 and 0.40 s, respectively) compared to the value of the backbone methylene carbons of the molecule.

At least two components contribute to the line-shape of each of the carbon resonances of the non-crystalline region, the line-shape of the amorphous region and that of the interphase. The interphase is a region where the molecules leaving the ordered crystalline phase gradually lose their crystalline conformation. During the course of crystallization, the hexyl branches are rejected from the crystal, and the branch concentration in this diffuse boundary is presumed to be higher than in the amorphous phase. Hence, the T_{1C} of carbons in the interphase may differ from the value in the more disordered amorphous phase or in the crystal (backbone CH₂). Since the relaxation curves of all the carbons were fitted with a single exponential function, it is concluded that, either the T_{1C} values of the interphase and amorphous are the same, as suggested in some works [29], or the value of the interface is significantly higher as it was concluded in other studies [30]. A T_{1C} value higher than 3 s for the backbone CH₂ in the interphase will be undetected in our experiments. Although the interfacial content may be high in the copolymer studied, when compared with the crystallinity level, it is most probably significantly lower than the amorphous fraction. Hence, within the time delays of our experiment, the relaxation will be dominated by the carbons of the amorphous region. Curve fitting to separate the line-shape of the interfacial region from that of the pure amorphous region was not attempted. The procedure is subject to the choice of a given functionality for the line-shape of each peak (not necessarily Lorentzian for the interface) and, in addition, the number of peaks, or components, needs to be specified a priori.

It is also of interest to notice the somewhat lower T_{1C} of the copolymer's backbone methylenes (0.27 s) compared to the value for the non-crystalline carbons of linear polyethylene (0.35 \pm 0.01 s) [26]. This difference reflects the effect of the branches to the overall molecular conformation of the intercrystalline region of the copolymer. With increasing comonomer content, the average backbone carbon–carbon intermolecular distance of the non-crystalline region increases, as recently documented by the decrease in the position of the WAXS amorphous halo [31]. Thus, the higher segmental relaxation rate of the copolymer, compared to the linear chain is a result of the increased average intermolecular distance between carbons of the main chain, which in the amorphous random coil are separated by the hexyl branch. The increased free volume favors segmental mobility. These NMR results indicate that the spin–lattice segmental relaxations of the non-crystalline regions can be used to characterize changes in conformational properties of this region caused by the

addition of comonomer to the linear polyethylene chain. Further studies in this direction are in progress [32].

In summary, low amplitude ¹³C magnetization of the non-crystalline region of isotactic polypropylene is enhanced via a cp MAS-based pulse technique. The sequence was successfully used to probe the T_{1C} of soft regions of semi-crystalline iPP and the data compared with the T_{1C} of a purely atactic polypropylene. It was noticed that the mixed conformations of the isotactic molecule in the non-crystalline region average to the same segmental relaxation rate as the atactic molecule. The technique was also tested to obtain T_{1C} of the non-crystalline carbons of an ethylene–1-octene random copolymer. The hexyl branches lead to an increased average backbone C–C intermolecular distance of the non-crystalline regions compared to the linear polyethylene chain and therefore, to a higher backbone methylene segmental mobility. The contribution to the recovery of a transient NOE was successfully modeled by a double exponential function obtained from the Solomon equations. Values of the NOE factor, T_{1C} , and T_{1CH} are obtained from the fitting. The carbon spin–lattice relaxations obtained with the cp MAS based technique were the same as those obtained by classical inversion or saturation recovery methods which do not invoke cross-polarization.

Acknowledgements

Support of this work by the National Science Foundation, Polymer Program (DMR-0094485) is gratefully acknowledged. J.A. Blanco acknowledges a scholarship from Fundacion Repsol-YPF (Spain).

References

- [1] Axelson DE. Carbon-13 solid state NMR of semicrystalline polymers. Deerfield Beach, FL: VCH, 1986.
- [2] Axelson DE, Mandelkern L, Popli R, Mathieu P. *J Polym Sci, Polym Phys Ed* 1983;21:2319.
- [3] Torchia DA. *J Magn Reson* 1978;30:613.
- [4] McBrierty VJ, Packer KJ. Nuclear magnetic resonance in solid polymers. Cambridge: Cambridge University Press, 1993.
- [5] Kitamaru R, Horii F, Murayama K. *Macromolecules* 1986;19:636.
- [6] Saito S, Moteki Y, Nakagawa N, Horii F, Kitamaru R. *Macromolecules* 1990;23:3256.
- [7] Ando I, Yamanobe T, Sorita T, Komoto T, Satao H, Deguchi K, Imanari M. *Macromolecules* 1984;17:1955.
- [8] Moe NE, Qiu X, Ediger MD. *Macromolecules* 2000;33:2145.
- [9] VanderHart DL. *Macromolecules* 1979;12:1232.
- [10] Xu Z, Mays JW, Chen X, Hadjichristidis N, Schilling F, Bair HE, Pearson DS, Fetters LJ. *Macromolecules* 1985;18:2560.
- [11] Sakurai K, MacKnight WJ, Lohse DJ, Schulz DN, Sissano JA. *Macromolecules* 1994;27:4941.
- [12] Sehanobish K, Patel RM, Croft BA, Chum SP, Kao CI. *J Appl Polym Sci* 1994;51:887.
- [13] VanderHart DL, Alamo RG, Nyden MR, Kim MH, Mandelkern L. *Macromolecules* 2000;33:6078.
- [14] Bunn A, Cudby MEA, Harris RF, Packer KJ, Say BJ. *Polymer* 1982;23:694.

- [15] Alizadeh A, Richardson L, Xu J, McCarney S, Marand H, Cheung YW, Chum S. *Macromolecules* 1999;32:6221.
- [16] Naito A, Ganapathy S, Akasaka K, McDowell CA. *J Magn Reson* 1983;54:226.
- [17] Zhou J, Fu R, Hu JZ, Li L, Ye C. *Solid State Nucl Magn Reson* 1997;7:291.
- [18] Findlay A, Harris RK. *J Magn Reson* 1990;87:605.
- [19] Findlay A, Harris RC. *Magn Reson Chem* 1990;28:S104.
- [20] Zhou J, Fu R, Li L, Ye C. *Acta Phys Sin* 1994;43:1245.
- [21] Solomon I. *Phys Rev* 1955;99:559.
- [22] Komoroski RA, Mandelkern L. In: Brame Jr EG, editor. *Applications of polymer spectroscopy*. New York: Academic Press, 1978. p. 57.
- [23] Paukkeri R, Väänänen T, Lehtinen A. *Polymer* 1993;34:2488.
- [24] Blanco JA, Alamo RG., In preparation.
- [25] Gomez MA, Tanaka H, Tonelli AE. *Polymer* 1987;28:2227.
- [26] Komoroski RA, Maxfield J, Sakaguchi F, Mandelkern L. *Macromolecules* 1977;10:550.
- [27] Yoon DY, Flory PJ. *Faraday Discuss Chem Soc* 1979;68:288.
- [28] Hunter BK, Russell K, Scammell MV, Thompson SL. *J Polym Sci, Polym Chem Ed* 1984;22:1383.
- [29] Kuwabara K, Kaji H, Horii F, Bassett DC, Olley RH. *Macromolecules* 1997;30:7516.
- [30] Mc Faddin DC, Russell KE, Kelusky EC. *Polym Commun* 1986;27:204.
- [31] Simanke AG, Alamo RG, Galland GB, Mauler RS. *Macromolecules* 2001;34:6959.
- [32] Carrilero I, Simanke AG, Alamo RG. In preparation.